Development of a Two-axis Dual Pendulum Thrust Stand for Thrust Vector Measurement of Hall Thrusters

Naoki Nagao[1], Shigeru Yokota[2], Kimiya Komurasaki[3], and Yoshihiro Arakawa[4]
The University of Tokyo, Tokyo, 113-8656

A 2D dual pendulum thrust stand was developed to measure thrust vector of a Hall thruster without thermal effect. A thruster is mounted on a pendulum and gap sensors are mounted on the other. By measuring thrust from the displacement between two pendulums, a thermal drift effect is canceled out. Two crossover knife-edges enable the pendulums to swing in both main thrust direction and its transversal direction. Thrust calibration using a pulley and weight system showed that the measurement errors were less than 0.25 mN (1.4%) in the main thrust direction and 0.09 mN (1.4%) in its transversal direction. The vector angle of a steering Hall thruster was measured with the stand. The steering angle has liner relationship with $(\dot{m}_{\text{left}} - \dot{m}_{\text{right}})/(\dot{m}_{\text{left}} + \dot{m}_{\text{right}})$, which rate of change depends on only *B*. The results can be explained by the inclination of thrust generated by a half-room.

Nomenclature

B	=	magnetic induction
F	=	Lorentz force
I	=	current of the wire
l	=	magnetic circuit width
$\dot{m}$	=	mass flow rate
V_{d}	=	discharge voltage
α	=	steering angle
θ	=	angle between the axis and thrust generated by a half-room

I. Introduction

A Hall thruster is a promising thruster in the electric propulsion systems for an N/S station keeping and orbit transfer applications because its thrust efficiency is higher than those of other thrusters at the specific impulse in the range of 1500–2500 s[1)]. Recently, high-power Hall thrusters have been developed for application to orbit transfer application in many countries.[2-5)] In Japan, MELCO has been developing a thruster with 264 mN thrust with thruster input power of 4.56 kW[6)].

However, real-time thrust measurement of a high power Hall thruster is difficult because of a thermal effect such as an inclination of vacuum chamber and a thermal strain of stand parts such as pendulum arms by the thermal radiation from the plume. [7)]

In this study, a dual pendulum thrust stand was designed and developed in order to measure the thrust without the thermal effects. The stand has two pendulums: a thruster is loaded on a pendulum, while a gap sensor is loaded on the other. The thermal effect is canceled out between two pendulums because both pendulums are equally affected by the inclination and the thermal distortion. The stand is also able to measure thrust vectors by its crossover knife edges.

The performance of the stand was evaluated by thrust calibration using a pulley and weight system. The thrust of a Hall thruster was measured in order to verify if the thermal effect is negligible. Thrust vector was measured by this stand using a steerable Hall thruster which can change the vector by the gradient of the propellant in the acceleration channel.

[1] Graduate student, Department of Aeronautics and Astronautics.
[2] Graduate student, Department of Aeronautics and Astronautics, yokota@al.t.u-tokyo.ac.jp.
[3] Associate Professor, Department of Advanced Energy, komurasaki@k.u-tokyo.ac.jp.
[4] Professor, Department of Aeronautics and Astronautics, arakawa@al.t.u-tokyo.ac.jp.

II. Experimental Setup

A. Two-axis dual pendulum thrust stand

Figure 1 depicts a schematic diagram of the 2D dual pendulum thrust stand, which comprises inner and outer pendulums, a thrust mount, a sensor mount, an actuator, and a calibration system. Two cross-over knife-edges support the pendulum arms: one is put on the other at a right angle (Fig. 2). These supporting points enable the pendulums to swing in the main thrust direction and in its transversal direction. The thruster mount is set on the inner pendulum. The outer pendulum is a reference. All effects such as the vacuum chamber inclination and the thermal drift, except for thrust, are cancelled by measuring the displacement between the two pendulums.

Displacements in the main thrust and transversal directions are measured using LED sensors, which are unaffected by electric and magnetic fields generated by Hall thruster operation.

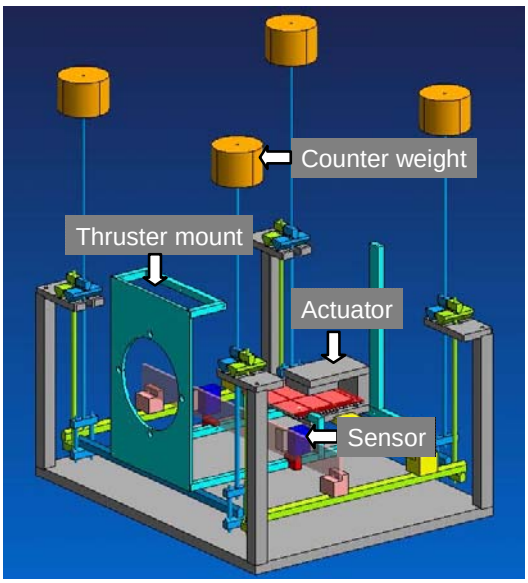

Figure 1. Schematic diagram of the 2D dual pendulum thrust stand.

Counterweights are installed only on the inner pendulum to enhance sensitivity. The electromagnetic actuator controls the pendulums to keep their displacements constant. Therefore, the actuating forces are equivalent to the thrusts. That equivalence contributes to the reduction in friction effects by wires and tubes, which are connected to a thruster for the supply of power, propellant, and cooling water.

Figure 3 shows that the electromagnetic actuator comprises two copper wires on the inner pendulum and a magnetic circuit consists of permanent magnets and iron yokes on the outer pendulum. Two orthogonal wires enable the actuator to generate Lorentz force $F=BIl$ in the main thrust direction and its transversal direction independently. Also, I is regulated via PID control[10] using a LabVIEW™ system.

Thrust was calibrated using a pulley and weight system. Three weights of 1 g each are used. The load was applied simultaneously in both main thrust direction and its transversal direction by setting the load direction at 20 deg with respect to the thruster axis.

B. Steerable Hall Thruster

Figure 4 shows a schematic diagram of the 0.5-kW-class magnetic layer type Hall thruster[8] developed at the University of Tokyo, which generates about 20 mN thrust. The thruster mass is about 3.8 kg. The inner and outer diameters of the acceleration channel are 48 and 62 mm, respectively. An acceleration channel wall was made of BN. The anode is located at 21 mm, upstream end of the acceleration channel. A solenoid coil is set at the center of the

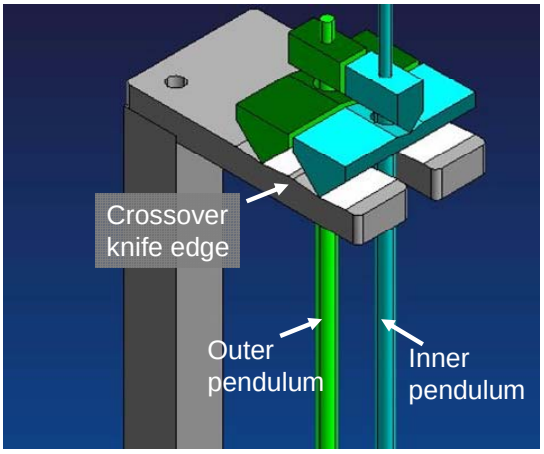

Figure 2. Crossover knife edge.

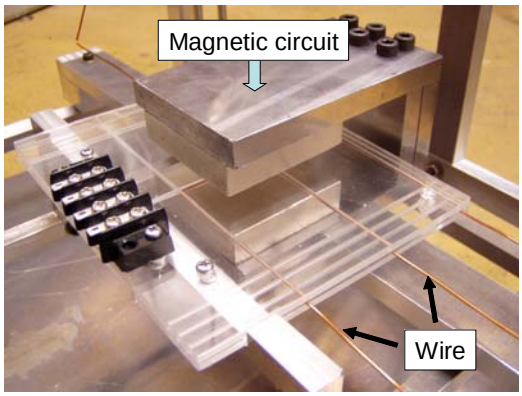

Figure 3. Actuator comprising wires and a layer-type Hall magnetic circuit.

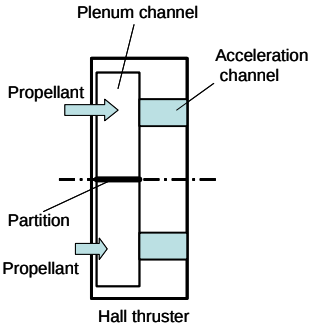

Figure 5. Propellant supply system with a segmented plenum channel.

thruster to apply a radial magnetic field in the acceleration channel. The magnetic flux density is varied by changing the coil current. There is no outer coil because a uniform magnetic field distribution is maintained along the azimuthal direction. A hollow cathode was used as a neutralizer.

A plenum channel is usually equipped immediately upstream of the anode surface to distribute a propellant gas uniformly into an annular acceleration channel. However, for this study, the plenum channel was separated into right and left rooms with walls to create a propellant density gradient from right to left or the reverse in the acceleration channel. Propellant flow rates were regulated using two mass flow controllers (Fig. 5). Operation parameters are discharge voltage, magnetic flux density, and total mass flow rate.

III. Result and Discussion

A. Thrust Calibration

Figures 6 shows the thrust signals in the main thrust direction (a) and its transversal direction (b). The averages of five measurements show good linearity. The measurement error was evaluated using the R.M.S. of difference from the fitted value.

Results show that the error was less than 0.25 mN (2.1%) in the main thrust direction and 0.09 mN (1.4%) in its transversal direction.

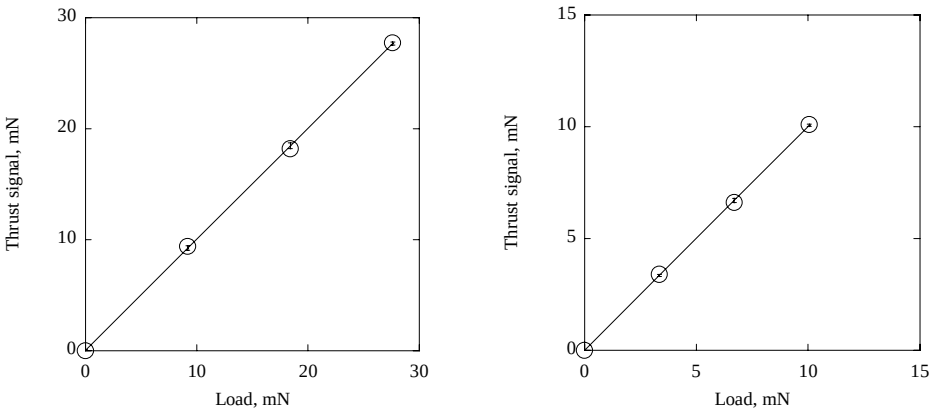

(a) main thrust direction **(b) transversal direction**

Figure 6 Thrust signals of the calibration.

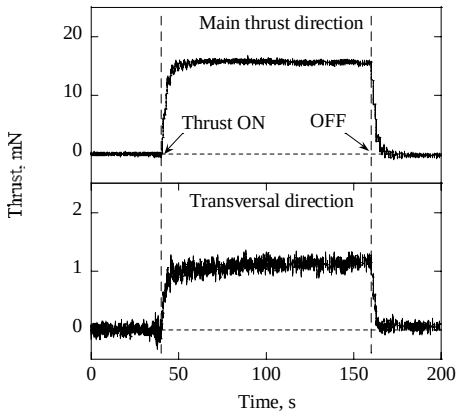

Figure 7. Thrust history during an operation.

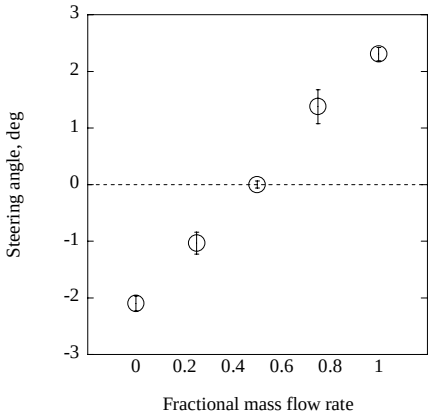

Figure 8. Steering angle of the thrust vector against the fractional mass flow rate (V_d=300 V, B=15 mT, m_{total}=13.9sccm).

B. 2D Thrust Measurement

Figure 7 shows the thrust history during operation. As this figure shows, thermal drift is negligibly small. Figure 8 shows the thrust angle as a function of $(\dot{m}_{left} - \dot{m}_{right})/(\dot{m}_{left} + \dot{m}_{right})$, where $\dot{m}_{right}$ and $\dot{m}_{left}$ respectively denote the mass flow rates from the right and left parts of the plenum channel. The total mass flow rate $\dot{m}_{left} + \dot{m}_{right}$ is fixed at the above-mentioned value during the experiment. The average values and errors of five measurements are shown in the figure. In this case, the maximum thrust vector deviation was ±4.6 deg; the measurement error was estimated at ±0.2 deg. Figures 9, 10, and 11 show the maximum steering angle as a function of B, V_d, and $\dot{m}_{total}$, respectively. As shown in these figures, the steering angle depends only on B.

These results are explained by the inclination of the thrust generated in a half-room as shown in the Fig. 12. The relation between α and θ is expressed as

$$a \simeq \tan a = \frac{(T_{right} - T_{left})\sin\theta}{(T_{right} + T_{left})\cos\theta} = \frac{(\dot{m}_{right} - \dot{m}_{left})}{(\dot{m}_{right} + \dot{m}_{left})}\tan\theta \simeq \theta\frac{(\dot{m}_{right} - \dot{m}_{left})}{(\dot{m}_{right} + \dot{m}_{left})}. \quad (1)$$

This equation describes the liner relation in Fig. 8. As shown in Fig. 9, α is changed by B, because B effects on the ionization region and magnetic field configuration, which can change θ. The other parameters have no effects on α because change of the other parameters canceled out in the term of $(\dot{m}_{left} - \dot{m}_{right})/(\dot{m}_{left} + \dot{m}_{right})$.

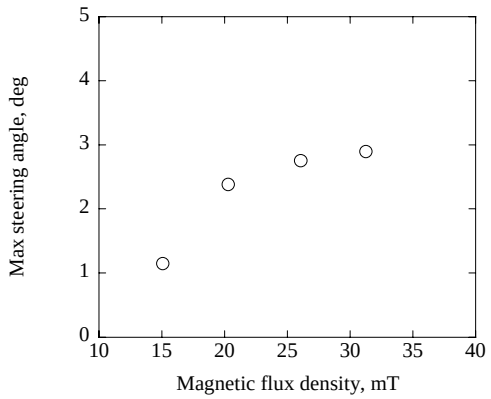

Figure 9. Max steering angle of the thrust vector as a function of magnetic flux density (V_d=300 V, m_{total}=13.9sccm).

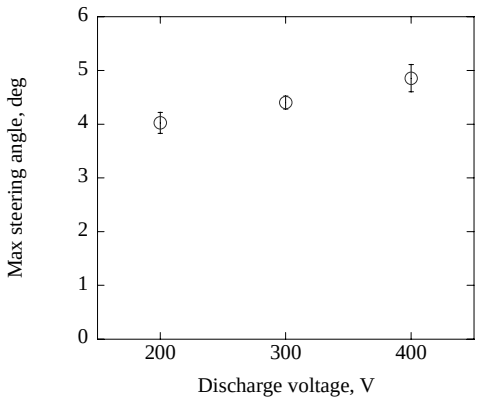

Figure 10. Max steering angle of the thrust vector as a function of discharge voltage (B=15 mT, m_{total}=13.9sccm).

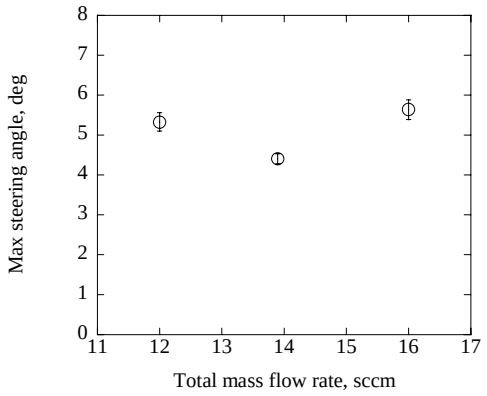

Figure 11. Steering angle of the thrust vector against the fractional mass flow rate (V_d=300 V, B=15 mT, m_{total}=13.9sccm).

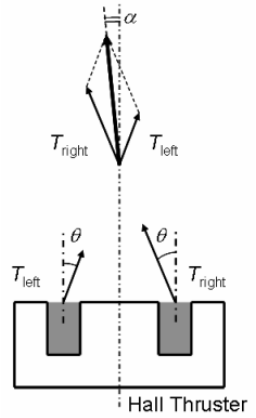

Figure 12. Relation between steering angle and ion beam angle.

IV. Conclusion

The 2D dual pendulum thrust stand for Hall thrusters was developed. The measurement performance of the stand is evaluated by thrust calibration using a pulley and weight system. As a result, the measurement error was 0.25mN (2.1%) in the main direction and 0.09 mN (1.4%) in the transversal direction.

Thrust vector angle of the steerable Hall thruster was measured with the 2D dual pendulum thrust stand. Thrust signal shows that the thermal effect of the stand is negligible. The steering angle has liner relationship with $(\dot{m}_{\text{left}} - \dot{m}_{\text{right}})/(\dot{m}_{\text{left}} + \dot{m}_{\text{right}})$, which rate of change depends on only B. The results can be explained by the inclination of thrust generated by a half-room.

Acknowledgments

The present work was supported by a Gran-in-Aid for Scientific Research (S), No.16106012 sponsored by Japan society for the promotion of science.

References

[1] H. R. Kaufman, “Technology of Closed-Drift Thrusters,” AIAA Journal **23**(1), 78–86 (1985).

[1] A. I. Morozov, “Stationary plasma thruster (SPT), development steps and, future perspectives,” IEPC-93-101, pp.945–949.

[2] A. I. Morozov, “Electric propulsion thrusters and plasmadynamics,” IEPC-95-05, pp.41–53.

[3] D. Manzella et al., “Laboratory Model 50 kW Hall Thruster,” AIAA-Paper-2002-3676, July, 2002.

[4] D. Milligan, D. Gestal, O. Camino, D. Estublier, and C. Koppel, “SMART-1 Electric Propulsion Operations,” AIAA-2004-3436.

[6] T. Ozaki, Y. Kasai, Y. Inanaga, T. Nakagawa, H. Osuga, T. Itoh, K. Kajiwara, and K. Matsui, “Electric propulsion Development Activity at MELCO,” AIAA-Paper-2006-4321, July, 2006.

[7] T. W. Haag, “Thrust stand for high-power electric propulsion devices,” Rev. Sci. Instrum. **62**(5), 1186–1191 (1991).

[5] J. K. Koester, J. B. McVey and E. J. Britt, “The Optimal Control of Thrust Vector of Hall-thrusters,” IEPC-99-123.

[8] N. Yamamoto, K. Komurasaki and Y. Arakawa, "Discharge Current Oscillation in Hall Thrusters," Journal of Propulsion and Power **21**(5), 870–876 (2005).